

2 **Neutrino-Induced-Muon Momentum Determination**
3 **by Multiple Coulomb Scattering in the MicroBooNE**
4 **LArTPC**

5 **The MicroBooNE Collaboration**

6 **ABSTRACT:** Liquid argon time projection chambers (LArTPCs) are an important detector technol-
7 ogy for neutrino physics. This technology provides precise three-dimensional reconstruction of
8 charged particle tracks that traverse the detector medium. We discuss a technique for measuring
9 a charged particle's momentum by means of multiple Coulomb scattering (MCS) in the Micro-
10 BooNE LArTPC, which does not require the full particle ionization track to be contained inside of
11 the detector volume as other track momentum reconstruction methods do (range-based momentum
12 reconstruction and calorimetric momentum reconstruction). We motivate use of this technique,
13 prescribe a tuning of the underlying theory formula, quantify its performance on fully contained
14 beam-neutrino-induced muon tracks both in simulation and in data, and quantify its performance
15 on exiting muon tracks in simulation. We find agreement between data and simulation for con-
16 tained tracks, with small bias in the momentum reconstruction and with resolutions that vary as
17 a function of track length, decreasing from about 10% for the shortest (one meter long) tracks to
18 5% for longer (several meter) tracks. For exiting muons with at least one meter of track contained,
19 we find similarly small bias, and a resolution which is better than 15% for muons with momentum
20 below 2 GeV though worse at higher momenta due to detector resolution effects.

21	Contents	
22	1 Introduction and Motivation	1
23	2 Multiple Coulomb Scattering (MCS)	3
24	2.1 Tuning the Highland Formula for Argon	4
25	3 MCS Implementation Using the Maximum Likelihood Method	6
26	3.1 Track Segmentation and Scattering Angle Computation	6
27	3.2 Maximum Likelihood Theory	7
28	3.3 Maximum Likelihood Implementation	7
29	4 Range-based Energy Validation from Simulation	8
30	5 MCS Performance on Beam Neutrino-Induced Muons in MicroBooNE Data	8
31	5.1 Input Sample	8
32	5.2 Event Selection	9
33	5.3 Highland Validation	10
34	5.4 MCS Momentum Validation	10
35	6 MCS Performance on Existing Muons in MicroBooNE Simulation	12
36	7 Conclusions	13

37 **1 Introduction and Motivation**

38 MicroBooNE (Micro Booster Neutrino Experiment) is an R&D experiment based at the Fermi Na-
39 tional Accelerator Laboratory (Fermilab) that uses a large Liquid Argon Time Projection Chamber
40 (LArTPC) to investigate the excess of low energy events observed by the MiniBooNE experiment
41 [1] and to study neutrino-argon cross-sections. MicroBooNE is part of the Short-Baseline Neutrino
42 (SBN) physics program, along with two other LArTPCs: the Short Baseline Near Detector (SBND)
43 and the Imaging Cosmic And Rare Underground Signal (ICARUS) detector. MicroBooNE also per-
44 forms important research and development in terms of detector technology and event reconstruction
45 techniques for future LArTPC experiments including DUNE (Deep Underground Neutrino Exper-
46 iment).

47
48 The MicroBooNE detector[2] consists of a rectangular time projection chamber (TPC) with
49 dimensions 2.6 m width \times 2.3 m height \times 10.4 m length located 470 m away from the Booster
50 Neutrino Beam (BNB) target. LArTPCs allow for precise three-dimensional reconstruction of par-
51 ticle interactions. The x - direction of the TPC corresponds to the drift coordinate, the y - direction
52 is the vertical direction, and the z - direction is the direction along the beam. The mass of active

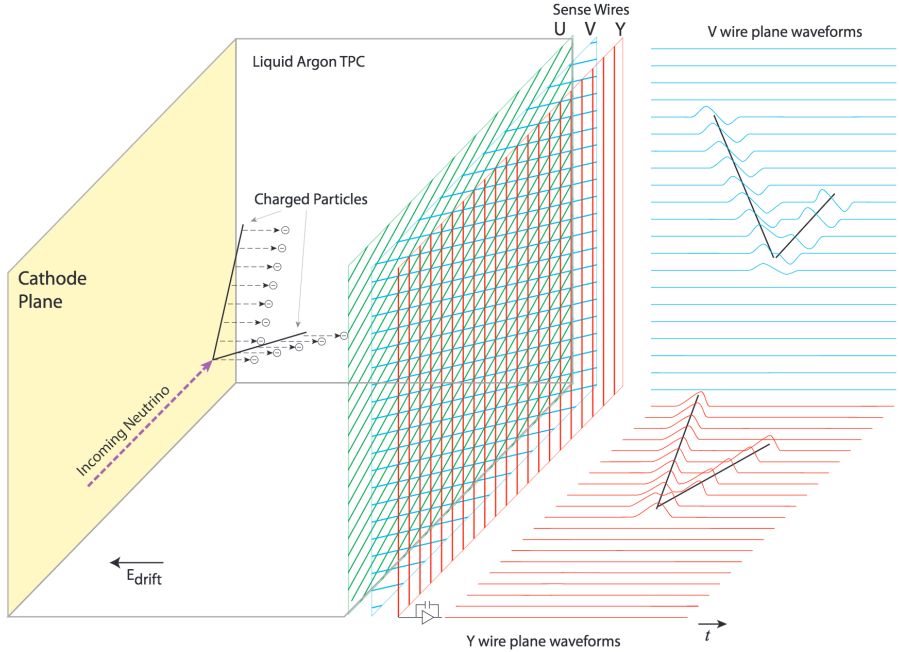


Figure 1. A diagram of the time projection chamber of the MicroBooNE detector [3]. PMTs (not shown) are located behind the wire planes.

53 liquid argon in the MicroBooNE TPC is 89 tons, with the total cryostat containing 170 tons of
 54 liquid argon.

55

56 A set of 32 photomultiplier tubes (PMTs) and three wire planes with 3 mm spacing at angles
 57 of 0, and ± 60 degrees with respect to the vertical are located in the TPC for event reconstruction
 58 (Figure 1). The cathode plane operating voltage is -70 kV. In a neutrino interaction, a neutrino from
 59 the beam interacts with an argon nucleus and the charged outgoing secondary particles traverse the
 60 medium, losing energy and leaving an ionization trail. The resulting ionization electrons drift to the
 61 anode side of the TPC, containing the wire planes. The passage of these electrons past the first two
 62 wire planes induces a signal in them, and their collection on the third plane also generates a signal.
 63 These signals are used to create three distinct two-dimensional views (in terms of wire and time)
 64 of the event. Combining these wire signals with timing information from the PMTs allows for full
 65 three-dimensional reconstruction of the event. The fiducial volume used in this analysis is defined
 66 as the full TPC volume reduced by 20 cm from both the cathode plane and the anode wire planes,
 67 by 26.5 cm from both the top and bottom walls of the TPC, by 20 cm from the beam-upstream wall
 68 of the TPC, and by 36.8 cm from the beam-downstream wall of the TPC, which corresponds to a
 69 mass of 55 tons. This fiducial volume was chosen to reduce the impact of electric field nonuniformities
 70 near the edges of the TPC.

71

72 The Booster Neutrino Beam (BNB) is predominantly composed of muon neutrinos (ν_μ) with
 73 a peak neutrino energy of about 0.7 GeV, some of which undergo charge-current (ν_μ CC) interac-
 74 tions in the TPC and produce muons. For muon tracks that are completely contained in the TPC, it
 75 is straightforward to calculate their momentum with a measurement of the length of the particle's
 76 track, or with calorimetric measurements which come from wire signal measurements. However,
 77 around half of muons from BNB ν_μ CC interactions in MicroBooNE are not fully contained in the
 78 TPC, and therefore using length-based calculations for these uncontained tracks is not a possibil-
 79 ity. The only way to compute the energy of a non-contained three-dimensional track is by means
 80 of multiple Coulomb scattering (MCS).

81
 82 In this paper we describe the theory behind multiple Coulomb scattering and a maximum
 83 likelihood based algorithm that is used to determine the momentum of particles in a LArTPC.
 84 That this technique works and is valid for a sample of fully contained muons from BNB ν_μ CC
 85 interactions is demonstrated, with bias and resolutions quantified. Additionally, quantification of
 86 performance on exiting tracks is presented.

87 2 Multiple Coulomb Scattering (MCS)

88 Multiple Coulomb scattering (MCS) occurs when a charged particle enters a medium and under-
 89 goes electromagnetic scattering with atomic nuclei. This scattering perturbs the original trajectory
 90 of the particle within the material (Figure 2). For a given energy, the angular deflection scatters of
 91 a particle in either the x' direction or y' direction (as indicated in the aforementioned figure) form
 92 a Gaussian distribution centered at zero with a width, σ_o^{HL} given by the Highland formula [4]:

$$\sigma_o^{HL} = \frac{13.6 \text{ MeV}}{p\beta c} z \sqrt{\frac{\ell}{X_0}} \left[1 + 0.0038 \times \ln\left(\frac{\ell}{X_0}\right) \right] \quad (2.1)$$

93 where β is the ratio of the particle's velocity to the speed of light assuming the particle is a muon,
 94 ℓ is the distance traveled inside the material, z is the magnitude of the charge of the particle, and
 95 X_0 is the radiation length of the target material (taken to be a constant 14 cm in liquid argon). In
 96 practice, a modified version of the Highland formula is used

$$\sigma_o = \sqrt{(\sigma_o^{HL})^2 + (\sigma_o^{res})^2} = \sqrt{\left(\frac{13.6 \text{ MeV}}{p\beta c} z \sqrt{\frac{\ell}{X_0}} \left[1 + 0.0038 \ln\left(\frac{\ell}{X_0}\right) \right] \right)^2 + (\sigma_o^{res})^2} \quad (2.2)$$

97 where the formula is “modified” from the original Highland formula (Equation 2.1) in that it in-
 98 cludes a detector-inherent angular resolution term, σ_o^{res} . For this analysis, this term is given a fixed
 99 value of 3 mrad which has been determined to be an acceptable value based on simulation studies
 100 of higher momenta muons. Equation 2.1 predicts an RMS angular scatter of 3 mrad at around
 101 4.5 GeV muon momentum when $\ell \approx X_0$ as is the case in this study; the fully contained muons
 102 addressed in this analysis have momenta below 1.5 GeV making detector resolution negligible.

103
 104 With the Highland formula, the momentum of a track-like particle can be determined using
 105 only the 3D reconstructed track it produces in the detector, without any calorimetric or track range

106 information. Within neutrino physics, past emulsion detectors like the DONUT [5] and OPERA [6]
 107 experiments have used MCS to determine particle momenta. Additionally, the MACRO [7] experi-
 108 ment at Gran Sasso Laboratory utilized this technique as well. While the original method for using
 109 MCS to determine particle momentum in a LArTPC used a Kalman Filter and was described by the
 110 ICARUS collaboration [8] (more recently the ICARUS collaboration describes another method[9]),
 111 the maximum-likelihood based method discussed in this paper for use in the MicroBooNE detector
 112 is described in detail in Section 3.

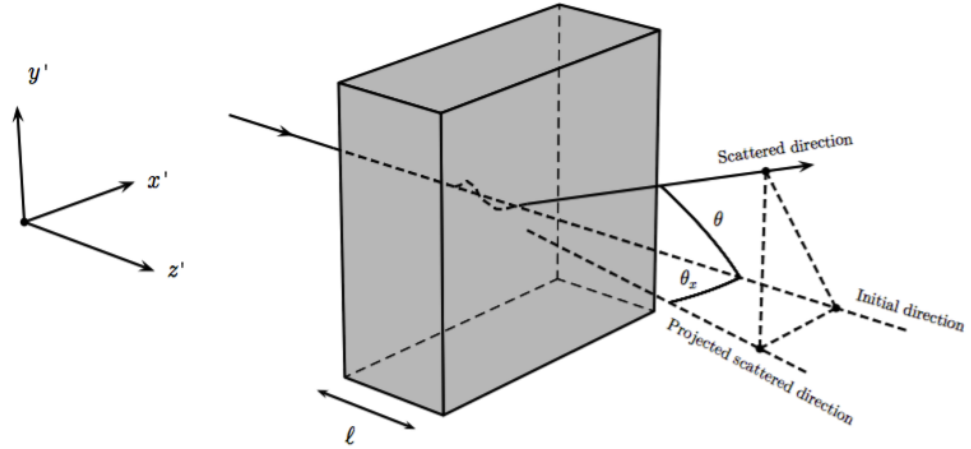


Figure 2. The particle’s trajectory is deflected as it traverses through the material.

113 2.1 Tuning the Highland Formula for Argon

114 The Highland formula as written in Equation 2.1 originated from a 1991 publication by G. R. Lynch
 115 and O. I. Dahl[10]. The constants in the equation (13.6 and 0.0038) were determined using a fit to
 116 “singly charged heavy particles for 14 different elements and 7 different thicknesses ranging from
 117 10^{-4} radiation lengths to 100 radiation lengths.” All of the simulated particles were relativistic,
 118 with $\beta = 1$. The materials in which they studied scattering ranged from hydrogen (with Z=1) to
 119 uranium (with Z=92). Given that the constants in the formula were determined from a fit to a wide
 120 range of Z with a wide range of material thicknesses, there is reason to believe that these constants
 121 should differ for scattering specifically in liquid argon with $l \approx X_0$. There is also reason to believe
 122 that these constants might change for particles with $\beta < 1$, which is the case for portions of con-
 123 tained muons in this analysis.

124

125 In order to re-tune these constants to liquid argon, a large sample of muons were simulated
 126 with GEANT4[11] in the MicroBooNE TPC and their true angular scatters were used in a fit, with
 127 $l = X_0$. The reason for using $l = X_0$ is that the Highland equation simplifies to remove dependence
 128 on the 0.0038 constant:

$$\sigma_o = \frac{13.6 \text{ MeV}}{p\beta c} \quad (2.3)$$

129 The 13.6 constant in Equation 2.3 was fit for as a function of true muon momentum for each
 130 scatter, in order to explore the β dependence of this constant. The fitted constant value as a function
 131 of true momentum is shown in Figure 3.

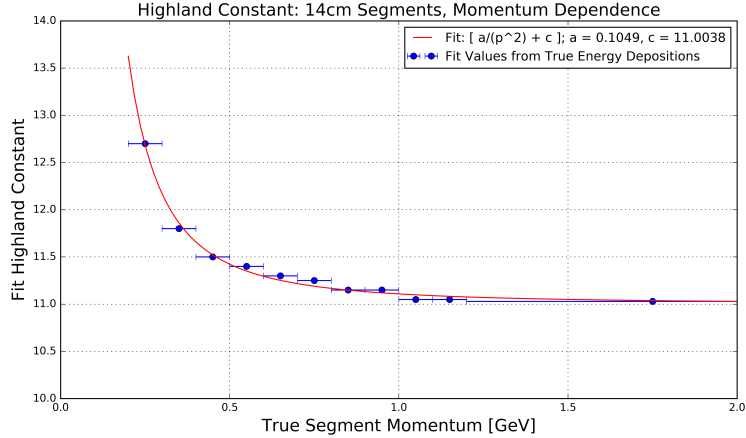


Figure 3. Fitted Highland constant as a function of true segment momentum for $l = X_0$ simulated muons in the MicroBooNE LArTPC. Blue x- error bars indicate true momentum bin width with data points drawn at the center of each bin. Shown in red is a fit to these data points with functional form $\frac{a}{p^2} + c$, with converged values for floating constants a and c shown in the legend.

132 It can be seen that the fitted value is always less than the nominal 13.6 and asymptotically
 133 approaches a constant at higher momentum (where $\beta = 1$) of about 11.0. The value increases in
 134 the momentum region where $\beta < 1$. Shown in red is a fit to these data points with functional form
 135 $\frac{a}{p^2} + c$, with converged values for floating constants a and c being 0.1049 and 11.0038 respectively.
 136 This functional form was chosen because it fit the data well, and asymptotically approaches a
 137 constant value when β approaches 1. This function will henceforth be referred to as $\kappa(p)$:

$$\kappa(p) = \frac{0.1049}{p^2} + 11.0038 \quad (2.4)$$

138 In this analysis, $\kappa(p)$ is used as a replacement for the 13.6 constant in the Highland formula.
 139 To visualize the Highland formula for $l = X_0$ both before and after the $\kappa(p)$ replacement, see Figure
 140 4. It is recommended that future LArTPC experiments use this parameterization of the Highland
 141 formula, or at the very least conduct their own studies to tune the Highland formula for scattering
 142 specifically in argon.

144 The form of the Highland equation used in this analysis is therefore given by Equation 2.2, with
 145 13.6 replaced by $\kappa(p)$ given by Equation 2.1, noting that with segmentation length $\ell = X_0 = 14\text{cm}$
 146 the formula simplifies to remove dependence on the 0.0038 constant. For the sake of readability,
 147 the formula simplifies to remove dependence on the 0.0038 constant. For the sake of readability,
 148 Equation 2.2 is rewritten here:

$$\sigma_o^{RMS} = \sqrt{(\sigma_o)^2 + (\sigma_o^{res})^2} = \sqrt{\left(\frac{\kappa(p)}{p\beta c} z \sqrt{\frac{\ell}{X_0}} \left[1 + 0.0038 \ln\left(\frac{\ell}{X_0}\right)\right]\right)^2 + (\sigma_o^{res})^2} \quad (2.5)$$

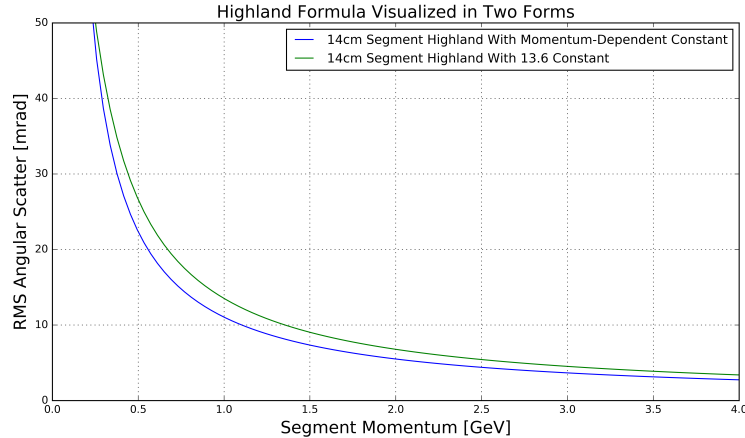


Figure 4. The Highland scattering RMS σ_o for 14 cm segment lengths and 0 detector-inherent angular resolution as a function of true momentum before and after retuning. In green is shown Equation 2.3 (using 13.6 constant) and in blue is the same equation replacing 13.6 with $\kappa(p)$.

149 3 MCS Implementation Using the Maximum Likelihood Method

150 This section describes exactly how the phenomenon of multiple Coulomb scattering is leveraged
 151 to determine the momentum of a muon track reconstructed in a LArTPC. In general, the approach
 152 is as follows:

- 153 1. The three-dimensional track is divided into segments of configurable length.
 - 154 2. The scattering angles between consecutive segments are measured.
 - 155 3. Those angles combined with the modified, tuned Highland formula (Equation 2.5) are used
 156 to build a likelihood that the particle has a specific momentum, taking into account energy
 157 loss in upstream segments of the track.
 - 158 4. The momentum corresponding to the maximum likelihood is chosen to be the MCS com-
 159 puted momentum.
- 160 Each of these steps are discussed in detail in the following subsections.
- 161

162 3.1 Track Segmentation and Scattering Angle Computation

163 Track segmentation refers to the subdivision of three-dimensional reconstructed trajectory points
 164 of a reconstructed track into portions of definite length. In this analysis, the tracks are automati-
 165 cally reconstructed by the “pandoraNuPMA” projection matching algorithm which constructs the
 166 three-dimensional trajectory points by combining two-dimensional hits reconstructed from signals
 167 on the different wire planes along with timing information from the photomultiplier tubes to re-
 168 construct the third dimension [12]. The segmentation routine begins at the start of the track, and
 169 iterates through the trajectory points in order, defining segment start and stop points based on the

170 straight-line distance between them. There is no overlap between segments. Given the subset of the
 171 three-dimensional trajectory points that correspond to one segment of the track, a three-dimensional
 172 linear fit is applied to the data points, weighting all trajectory points equally in the fit. In this analy-
 173 sis, a segment length of 14 cm is used, which is a tunable parameter that has been optimized based
 174 on simulation studies.

175
 176 With the segments defined, the scattering angles between the linear fits from adjacent segments
 177 are computed. A coordinate transformation is performed such that the z' direction is oriented along
 178 the direction of the linear fit to the first of the segment pair. The x' and y' coordinates are then
 179 defined such that all of x' , y' , and z' are mutually orthogonal, as shown in Figure 2. The scattering
 180 angles both with respect to the x' direction and the y' direction are then computed to be used by
 181 the MCS algorithm. Note that only the scattering angle with respect to the x' direction is drawn in
 182 Figure 2.

183 3.2 Maximum Likelihood Theory

184 The normal probability distribution for a scattering angle in either the x' or y' direction, $\Delta\theta$ with
 185 an expected gaussian error σ_o and mean of zero is given by:

$$f_X(\Delta\theta) = (2\pi\sigma_o^2)^{-\frac{1}{2}} \exp\left(-\frac{1}{2}\left(\frac{\Delta\theta}{\sigma_o}\right)^2\right) \quad (3.1)$$

186 Here, σ_o is the RMS angular deflection computed by the modified, tuned Highland formula
 187 (Equation 2.5), which is a function of both the momentum and the length of that segment. Since
 188 energy is lost between segments along the track, σ_o increases for each angular measurement along
 189 the track so we replace σ_o with $\sigma_{o,j}$, where j is an index representative of the segment.

190
 191 To get the likelihood, one takes the product of $f_X(\Delta\theta_j)$ over all n of the $\Delta\theta_j$ segment-to-
 192 segment scatters along the track. With some manipulation, this product becomes

$$L(\sigma_{o,1}, \dots, \sigma_{o,n}; \Delta\theta_1, \dots, \Delta\theta_n) = (2\pi)^{-\frac{n}{2}} \times \prod_{j=1}^n (\sigma_{o,j})^{-1} \times \exp\left(-\frac{1}{2} \sum_{j=1}^n \left(\frac{\Delta\theta_j}{\sigma_{o,j}}\right)^2\right) \quad (3.2)$$

193 In practice, rather than maximizing likelihood it is more computationally convenient to instead
 194 minimize the negative log likelihood. Inverting the sign and taking the natural logarithm of the
 195 likelihood L gives an expression that is related to a χ^2

$$-l(\mu_o; \sigma_{o,1}, \dots, \sigma_{o,n}; \Delta\theta_1, \dots, \Delta\theta_n) = -\ln(L) = \frac{n}{2} \ln(2\pi) + \sum_{j=1}^n \ln(\sigma_{o,j}) + \frac{1}{2} \sum_{j=1}^n \left(\frac{\Delta\theta_j}{\sigma_{o,j}}\right)^2 \quad (3.3)$$

196 3.3 Maximum Likelihood Implementation

197 Given a set of angular deflections in the x' and y' directions for each segment as described in
 198 Section 3.1 a raster scan over postulated track momenta in steps of 1 MeV up to 7.5 GeV is com-
 199 puted and the step with the smallest negative log likelihood (Equation 3.3) is chosen as the final
 200 MCS momentum. Note that Equation 3.3 includes a $\sigma_{o,j}$ term which changes for each consecutive
 201 segment because their energies are decreasing. The energy of the j th segment is given by

$$E_j = E_t - E_j^{\text{upstream}} \quad (3.4)$$

where E_j^{upstream} is the energy loss upstream of this segment, computed by integrating the muon stopping power curve given by the Particle Data Group (PDG)[14] along the length of track upstream of this segment. This definition of E_j therefore takes into account energy loss along the track. Note that Equation 3.4 introduces a minimum allowable track energy determined by the length of the track, as E_j must remain positive. This value of segment energy is converted to a momentum, p , with the usual energy-momentum relation assuming the muon mass, and is then used to predict the RMS angular scatter for that segment (σ_o) by way of Equation 2.5.

4 Range-based Energy Validation from Simulation

In order to quantify the performance of the MCS energy estimation method on fully contained muons in data, an additional handle on energy is needed. Here, range-based energy is used. The stopping power of muons in liquid argon is well described by the continuous-slowing-down-approximation (CSDA) by the particle data group (PDG) with agreement to data at the sub-percent level [13] [15] [16]. By using a linear interpolation between points in the cited PDG stopping power table, the length of a track can be used to reconstruct the muon’s total energy with good accuracy. A simulated sample of fully contained BNB neutrino-induced muons longer than one meter is used to quantify the bias and resolution for the range-based energy estimation technique. The range is defined as the straight-line distance between the true starting point and true stopping point of a muon. The bias and resolution are computed in bins of true total energy of the muons by fitting a gaussian to a distribution of the fractional energy difference ($\frac{E_{\text{Range}} - E_{\text{True}}}{E_{\text{True}}}$) in each bin. The mean of each gaussian indicates the bias for that true energy bin, and the width indicates the resolution. Figure 5 shows the bias and resolution for the range-based energy reconstruction method. It can be seen that the bias is negligible and the resolution for this method of energy reconstruction is on the order of 2-4%. Based on this figure, it is clear that range-based energy (and therefore range-based momentum) is a good handle on the true energy (momentum) of a reconstructed muon track in data, assuming that the track is well reconstructed in terms of length.

5 MCS Performance on Beam Neutrino-Induced Muons in MicroBooNE Data

5.1 Input Sample

The input sample to this portion of the analysis is $\sim 5 \times 10^{19}$ protons-on-target worth of triggered BNB neutrino interactions in MicroBooNE data, which is a small subset of the nominal amount of beam scheduled to be delivered to the detector. These events are run through a fully automated reconstruction chain which produces reconstructed objects including three-dimensional neutrino interaction points (vertices), three-dimensional tracks for each outgoing secondary particle from the interaction, and PMT-reconstructed optical flashes from the interaction scintillation light. The fiducial volume used in this analysis is defined in Section 1.

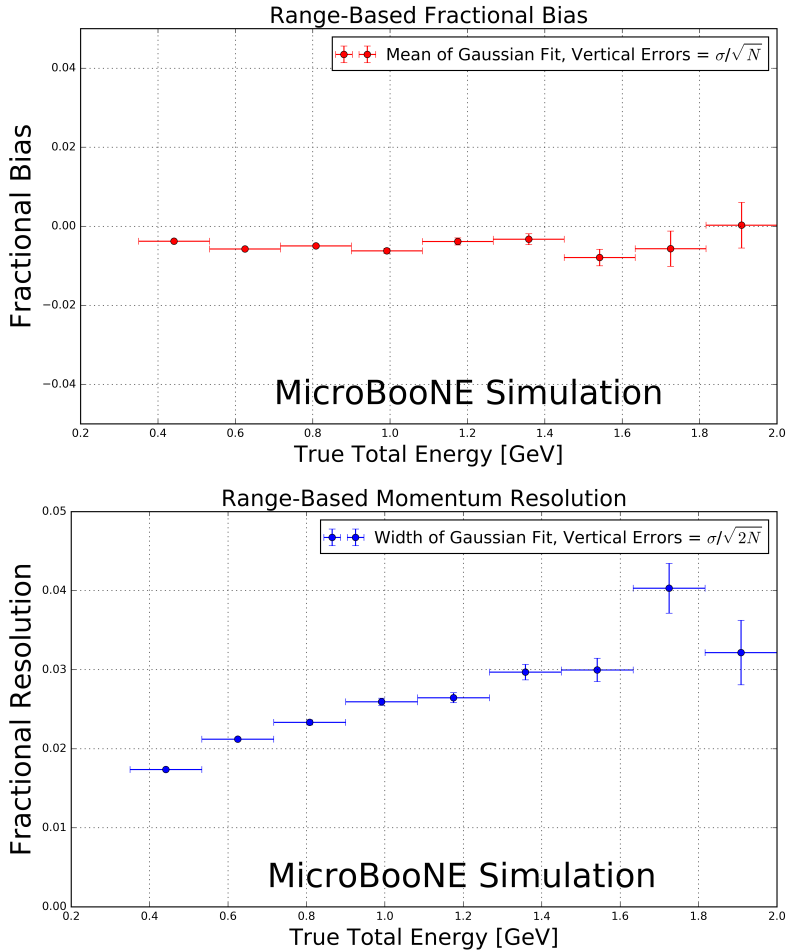


Figure 5. Range-based energy fractional bias (top) and resolution (bottom) from a sample of simulated fully contained BNB neutrino-induced muons using true starting and stopping positions of the track. The bias is less than 1% and the resolution is below $\approx 4\%$.

236 5.2 Event Selection

237 The following selection cuts are placed on the aforementioned reconstructed objects to select ν_μ
 238 charged-current interactions in which a candidate muon track exiting the interaction vertex is fully
 239 contained within the fiducial volume:

- 240 1. The event must have at least one bright optical flash in coincidence with the expected BNB
 241 neutrino arrival time.
- 242 2. Two or more reconstructed tracks must originate from the same reconstructed vertex within
 243 the fiducial volume.
- 244 3. The span in $z-$ of the track must be within 70 cm of the $z-$ position of the optical flash as
 245 determined by the pulse height and timing of signals in the 32 PMTs.

- 246 4. For events with exactly two tracks originating from the vertex, additional calorimetric-based
 247 cuts are applied to mitigate backgrounds from in-time cosmics which produce Michel elec-
 248 trons that are reconstructed as a track.
- 249 5. The longest track originating from the vertex is assumed to be a muon, and it must be fully
 250 contained within the fiducial volume.
- 251 6. The longest track must be at least one meter long, in order to have enough sampling points
 252 in the MCS likelihood to obtain a reasonable estimate of its momentum.

253 In this sample of MicroBooNE data, 598 events (tracks) remain after all event selection cuts.
 254 The relatively low statistics in this sample is due to the limited input sample, described in Sec-
 255 tion 5.1. Each of these events (tracks) were scanned by hand with a 2D interactive event display
 256 showing the raw wire signals of the interaction from each wire plane, with the 2D projection of the
 257 reconstructed muon track and vertex overlaid. The scanning was done to ensure the track was well
 258 reconstructed with start point close to the reconstructed vertex and end point close to the end of the
 259 visible wire-signal track in all three planes. Additionally the scanning was to remove obvious mis-
 260 identification (MID) topologies such as cosmic rays inducing Michel electrons at the reconstructed
 261 neutrino vertex which were not successfully removed by the automated event selection cuts. After
 262 rejecting events (tracks) based on hand scanning, 396 tracks remain for analysis.

263 5.3 Highland Validation

264 The Highland formula indicates that histograms of the track segment-by-segment angular devia-
 265 tions in both the x' and y' directions divided by the width predicted from the Highland equation
 266 σ_o^{HL} (Equation 2.5) should be gaussian with a width of unity. In order to calculate the momentum
 267 p in the Highland equation, p for each segment is computed with Equation 3.4 where E_t comes
 268 from the converged MCS computed momentum of the track. For each consecutive pair of segments
 269 in this sample of 396 tracks, the angular scatter in milliradians divided by the Highland expected
 270 RMS in milliradians is an entry in the area-normalized histogram shown in Figure 6. From this
 271 figure we can see that the basis of the MCS technique is validated.

272 5.4 MCS Momentum Validation

273 The MCS momentum versus range-based momentum for this sample of 396 tracks can be seen in
 274 Figure 7.

275 The MCS momentum fractional bias and resolution as a function of range-based momentum
 276 for this sample of 396 tracks is shown in Figure 8. In order to compute this bias and resolution,
 277 distributions of fractional inverse momentum difference ($\frac{p_{MCS}^{-1} - p_{Range}^{-1}}{p_{Range}^{-1}}$) in bins of range-based
 278 momentum p_{Range} are fit to gaussians and the mean of the fit determines the bias while the width
 279 of the fit determines the resolution for that bin. Inverse momentum is used here because the binned
 280 distributions are more gaussian (since the Highland formula measures inverse momentum in terms
 281 of track angles that have reasonably Gaussian errors). Note that simply using the mean and RMS of
 282 the binned distributions yields similar results. Also shown in this figure are the bias and resolutions
 283 for an analogous simulated sample consisting of full BNB simulation with CORSIKA-generated

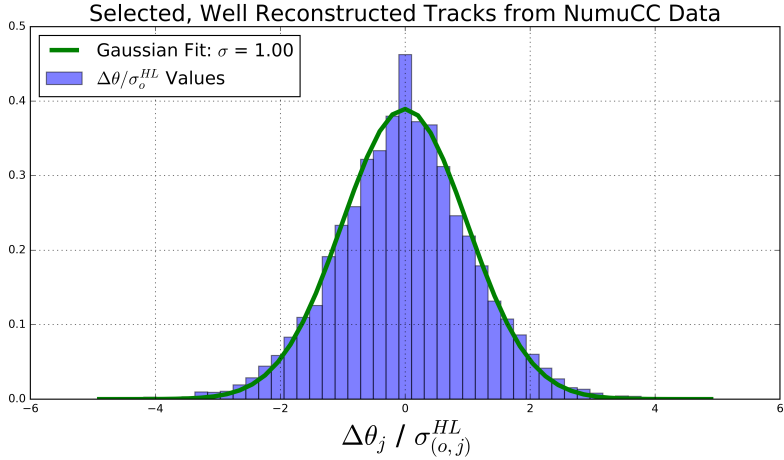


Figure 6. Segment-to-segment measured angular scatters in both the x' and y' directions divided by the Highland formula (Equation 2.1) predicted width σ_o^{HL} for the automatically selected beam neutrino-induced fully contained muon sample in MicroBooNE data after hand scanning to remove poorly reconstructed tracks and obvious mis-identification (MID) topologies. A Gaussian distribution with a width of unity indicates that the basis of the MCS technique is validated.

[17] cosmic overlays passed through an identical reconstruction and event selection chain. Rather than hand scanning this sample, true simulation information was used by requiring the longest reconstructed track matched well in terms of true starting and stopping point of the ν_μ CC muon. This removes any mis identifications or interference from the simulated cosmics.

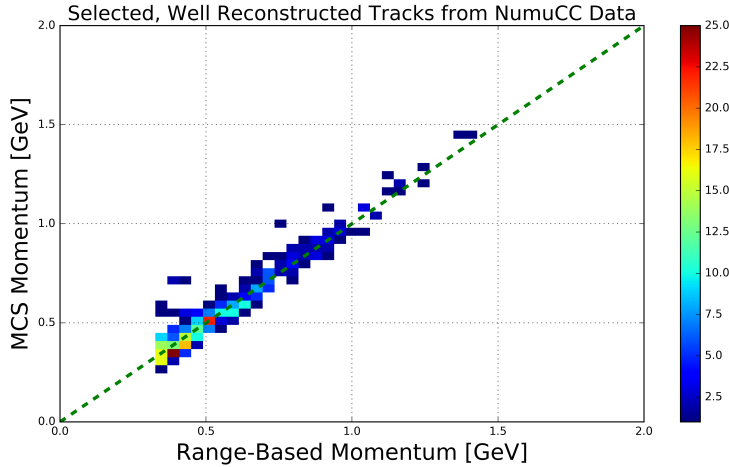


Figure 7. MCS computed momentum versus range momentum for the automatically selected beam neutrino-induced fully contained muon sample in MicroBooNE data after hand scanning to remove poorly reconstructed tracks and obvious mis-identification (MID) topologies.

Figure 8 indicates a bias in the MCS momentum calculation on the order of a few percent, with a resolution that decreases from about 10% (8%) for contained reconstructed tracks in data (simulation) with range momentum around 0.45 GeV (which corresponds to a length of about

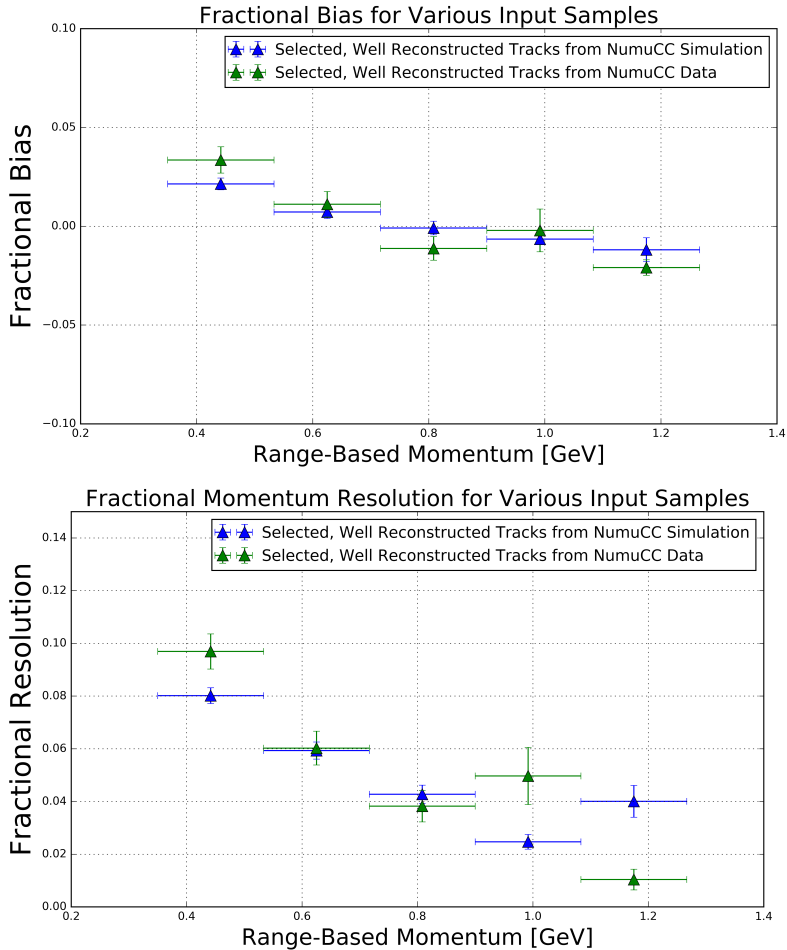


Figure 8. MCS momentum fractional bias (top) and resolution (bottom) for automatically selected contained ν_μ CC-induced muons from full simulated BNB events with cosmic overlay where the track matches with the true muon track (blue), and automatically selected contained ν_μ CC-induced muons from MicroBooNE data where the track is deemed well-reconstructed and likely-muon from hand scanning (green).

1.5 meters) to below 5% for contained reconstructed tracks in data and simulation with range momentum about 1.15 GeV (which corresponds to a length of about 4.6 meters). In general bias and resolutions agree between data and simulation within uncertainty.

6 MCS Performance on Exiting Muons in MicroBooNE Simulation

This section quantifies the MCS algorithm performance on a sample of simulated exiting muon tracks. The tracks are automatically reconstructed by the same “pandoraNuPMA” algorithm described in Section 3.1, and all tracks have at least one meter contained within the MicroBooNE TPC. This simulation does not include space charge effects which are non-negligible near the TPC walls.

300

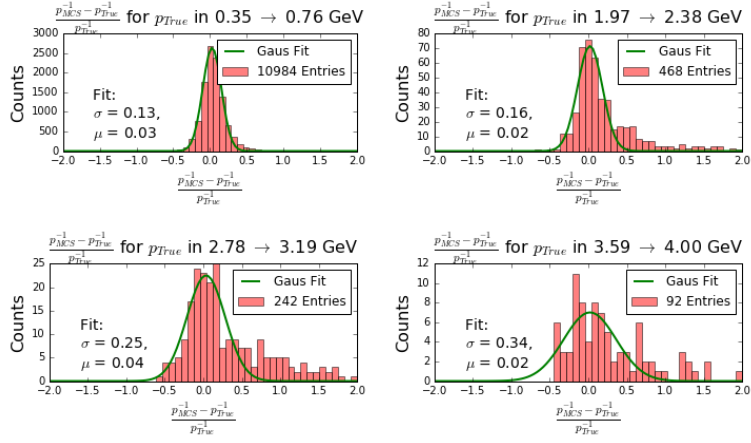


Figure 9. Fractional momentum difference for a few representative bins of true momentum.

301 The distribution of $(\frac{p_{MCS}^{-1} - p_{True}^{-1}}{p_{True}^{-1}})$ is shown for four representative bins of true momentum in
 302 Figure 9, along with the Gaussian fit to each. Low momentum tails in which the MCS momentum
 303 is an underestimation of the true momentum can be seen outside of the central gaussian fit. These
 304 tails can be attributed to reconstruction effects.

305
 306 The algorithm fractional bias and resolution as a function of true momentum are shown in Figure
 307 10. It can be seen that the bias is below 4% for all momenta, and the resolution is roughly 14%
 308 in the relevant momentum region for BNB ν_μ CC muons (below 2 GeV). The resolution worsens
 309 for muon momenta above this region because the angular scatters begin to be comparable with the
 310 detector resolution term of 3 mrad. Note that the resolution improves for longer lengths of track
 311 contained, with 10% resolution for muons below 2 GeV with more than 3.5 meters contained. Res-
 312 olution improving with length of track is intuitive; the longer portion of track contained, the more
 313 angular scattering measurements can be made to improve the likelihood.
 314

315 7 Conclusions

316 We have described a multiple Coulomb scattering maximum likelihood method for estimating the
 317 momentum of a three dimensional reconstructed track in a LArTPC and have provided motivation
 318 for development of such a technique. This technique is a very valuable tool; it is the only way to
 319 estimate the momentum of an exiting muon and will be an important ingredient in future oscillation
 320 and cross-section measurements by MicroBooNE and within the LArTPC community as a whole.
 321 The performance of this method has been quantified both in simulation and in data on beam ν_μ CC-
 322 induced muons which are fully contained, with fractional bias less than 3% and with fractional
 323 resolution at or below 10%. The performance of this method has been quantified on exiting muon
 324 tracks in simulation, with resolution better than 15% for muons in the relevant BNB energy region
 325 below 2 GeV.

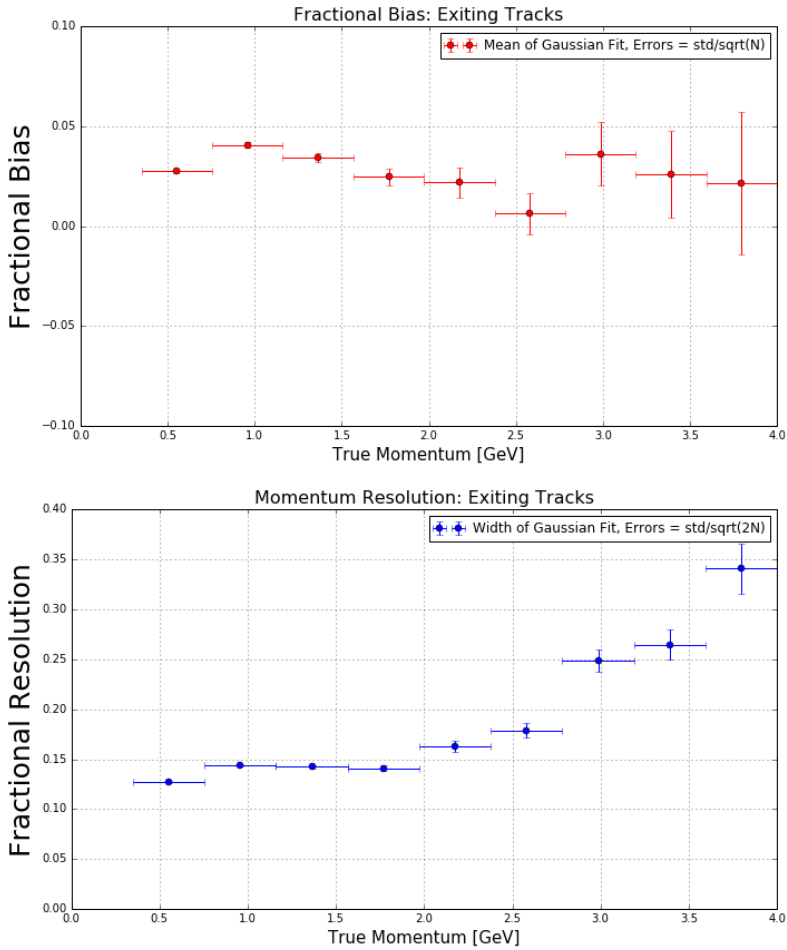


Figure 10. MCS momentum fractional bias (top) and resolution (bottom) as a function of true momentum from a sample of exiting reconstructed muon tracks.

326 References

- 327 [1] A. A. Aguilar-Arevalo *et al.* [MiniBooNE Collaboration], Improved Search for $\bar{\nu}_\mu \rightarrow \bar{\nu}_e$ Oscillations
328 in the MiniBooNE Experiment, Phys. Rev. Lett. **110**, 161801 (2013).
329 doi:10.1103/PhysRevLett.110.161801 [arXiv:1207.4809 [hep-ex], arXiv:1303.2588 [hep-ex]].
- 330 [2] R. Acciarri *et al.* [MicroBooNE Collaboration], “Design and Construction of the MicroBooNE
331 Detector,” arXiv:1612.05824 [physics.ins-det].
- 332 [3] S. Lockwitz, The MicroBooNE LArTPC,
333 <http://www-microboone.fnal.gov/talks/dpfMicroBooNELArTPC.pdf>.
- 334 [4] V. L. Highland, Some Practical Remarks on Multiple Scattering, Nucl. Instrum. Methods **129** (1975)
335 104-120.
- 336 [5] K. Kodama *et al.* [DONUT Collaboration], Phys. Lett. B **504**, 218 (2001)
337 doi:10.1016/S0370-2693(01)00307-0 [hep-ex/0012035].
- 338 [6] N. Agafonova *et al.* [OPERA Collaboration], New J. Phys. **14**, 013026 (2012)
339 doi:10.1088/1367-2630/14/1/013026 [arXiv:1106.6211 [physics.ins-det]].

- 340 [7] G. Giacomelli [MACRO Collaboration], Braz. J. Phys. **33**, 211 (2003)
341 doi:10.1590/S0103-97332003000200008 [hep-ex/0210006].
- 342 [8] A. Ankowski *et al.* [ICARUS Collaboration], “Measurement of through-going particle momentum by
343 means of multiple scattering with the ICARUS T600 TPC,” Eur. Phys. J. C **48**, 667 (2006)
344 doi:10.1140/epjc/s10052-006-0051-3 [hep-ex/0606006].
- 345 [9] M. Antonello *et al.*, “Muon momentum measurement in ICARUS-T600 LAr-TPC via multiple
346 scattering in few-GeV range,” arXiv:1612.07715 [physics.ins-det].
- 347 [10] G. R. Lynch and O. I. Dahl, Nucl. Instrum. Methods Section B (Beam Interactions with Materials
348 and Atoms) **B58**, **6** (1991).
- 349 [11] S. Agostinelli et al. Nucl. Instrum. Methods Phys. Res. **A506250-303** (2003)
- 350 [12] J. S. Marshall and M. A. Thomson, “The Pandora Software Development Kit for Pattern
351 Recognition,” Eur. Phys. J. C **75**, no. 9, 439 (2015) doi:10.1140/epjc/s10052-015-3659-3
352 [arXiv:1506.05348 [physics.data-an]].
- 353 [13] D. E. Groom, N. V. Mokhov and S. Striganov, “Muon Stopping Power and Range Tables: 10 MeV -
354 100 TeV” Table 5, <http://pdg.lbl.gov/2012/AtomicNuclearProperties/adndt.pdf>
- 355 [14] H. Bichsel, D. E. Groom, S.R. Klein, “Passage of Particles Through Matter” PDG Chapter 27, Figure
356 27.1 <http://pdg.lbl.gov/2005/reviews/passagerpp.pdf>
- 357 [15] Table 289: Muons in Liquid argon (Ar) http://pdg.lbl.gov/2012/AtomicNuclearProperties/MUON_ELOSS_TABLES/muonloss_289.pdf
- 358 [16] “Stopping Powers and Ranges for Protons and Alpha Particles,” ICRU Report No. 49 (1993); Tables
359 and graphs of these data are available at <http://physics.nist.gov/PhysRefData/>
- 360 [17] D. Heck, J. Knapp, J. N. Capdevielle, G. Schatz, T. Throw, *CORSIKA: A Monte Carlo Code to*
361 *Simulate Extensive Air Showers*, Forschungszentrum Karlsruhe Report FZKA 6019 (1998)